LASER
& PHOTONICS
REVIEWS

Laser Photonics Rev. **8,** No. 3, 443–449 (2014) / **DOI** 10.1002/lpor.201300189

Abstract Compact laser sources operating in mid infrared spectral region with stable emission are important for applications in spectroscopy and wireless communication. Quantum cascade lasers (QCL) are unique semiconductor sources covering mid infrared frequency range. Based on intersubband transitions, the carrier lifetime of these sources is in the ps range. For this reason their frequency response to direct modulation is expected to overcome the limits of standard semiconductor lasers. In this work injection locking of the roundtrip frequency of a QCL emitting at 9 μm is reported. Inter modes laser frequency separation is stabilized and controlled by an external microwave source. Designing an optical waveguide embedded in a microstrip line a flat frequency response to direct modulation up to 14 GHz is presented. Injection locking over MHz frequency range at 13.7 GHz is demonstrated. Numerical solutions of injection locking theory are discussed and presented as tool to describe experimental results.

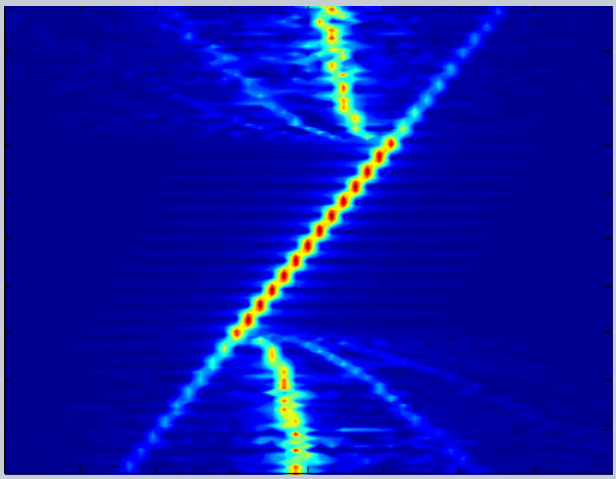

ORIGINAL
PAPER

Injection locking of mid-infrared quantum cascade laser at 14 GHz, by direct microwave modulation

Margaux Renaudat St-Jean[1], Maria Ines Amanti[1,*], Alice Bernard[1], Ariane Calvar[1], Alfredo Bismuto[2], Emilio Gini[2], Mattias Beck[2], Jerome Faist[2], H. C. Liu[3], and Carlo Sirtori[1]

1. Introduction

Injection locking is an experimental technique of synchronization of two coupled oscillators where one of the two is introduced as control signal for the second one. When the two oscillators work at a nearby frequency and their coupling is sufficiently strong, the control signal can capture, or lock, the second oscillator imposing its oscillation frequency. This concept is valid for any kind of self-sustained periodic oscillators such as clocks, electric circuits and lasers [1, 2]. Injection locking has been extensively exploited in laser diodes to either stabilize their emission frequency or the laser cavity modes separation. The latter corresponds to the stabilization of the round-trip frequency and it is normally achieved by injection of an external microwave signal directly on the driving current or through a small control in the cavity [3–5]. Tuning of the cavity modes separation in a specific frequency range around the free running value using this approach has also been reported [6]. However the ultimate frequency for direct modulation of interband laser is limited by relaxation oscillation dynamics [7]. To overcome this limitation optical injection locking is extensively exploited. This technique enables the improvement of the mode structure and noise behavior of a laser, by injection of the light of another laser with high stability [8].

Quantum cascade lasers (QCL) are unipolar sources based on intersubband transition with an ultrafast carrier lifetime (in the ps range). Predicted frequency bandwidths for these sources are in excess of tens of GHz, neglecting parasitic effects due to device packaging [9, 10]. Direct modulation of QCL is then a valid compact solution to gain the control of their round trip frequency. Moreover, the stabilization of the laser longitudinal modes is an enabling function with direct applications in wireless communication, metrology and active mode locking.

For THz QCL Gellie et al. [11] demonstrated injection locking of the inter mode frequency difference over hundreds of MHz by driving the laser bias with a microwave signal close to this frequency. Baryshev et al. [12] achieved the stabilization of the frequency difference between two lateral modes of a THz QCL by locking it to a microwave

[1] Laboratoire Matériaux et Phénomènes Quantiques, Université Paris Diderot—Paris 7, CNRS—UMR 7162, Bâtiment Condorcet 75205, Paris Cedex 13, France
[2] Institute of Quantum Electronics, ETH Zürich, CH-8093, Zürich, Switzerland
[3] Key Laboratory of Artificial Structures and Quantum Control, Department of Physics, Shanghai Jiao Tong University, Shanghai 200240, China
*Corresponding author: e-mail: maria.amanti@univ-paris-diderot.fr

reference; frequency locked linewidth of $\leq$10 Hz with negligible drift has been reported.

In the mid infrared, the spectral region of interest of this work, Paiella et al. [13] demonstrated broadening of the laser spectrum for a device emitting at 8 μm by direct modulation at the round trip frequency (11.7 GHz) but no stabilization of the cavity modes separation has been reported. More recently Hugi et al. [14] by direct modulation at 7.5 GHz of a broad band laser emitting at 7 μm demonstrate the tuning of the round-trip frequency over 65 kHz.

In this work we present the experimental and theoretical study of the direct modulation of a QCL emitting at 9 μm operating at nitrogen temperature. By employing a laser waveguide embedded in a microwave microstrip, injection locking of the round trip frequency of 13.7 GHz over MHz range is demonstrated. Experimental results are compared with the theory of injection locked systems.

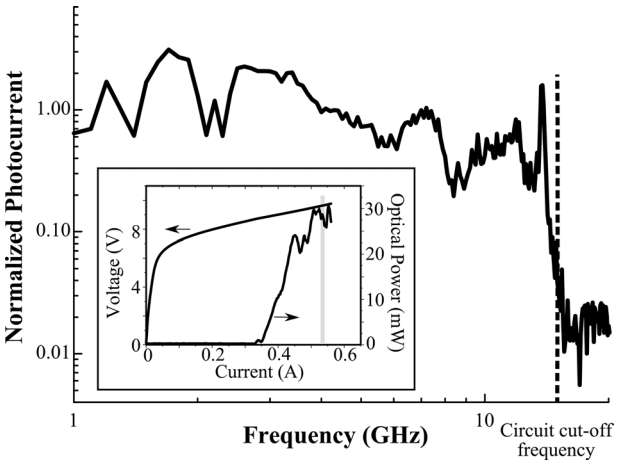

Figure 1 High frequency modulation response of a microstrip laser operating at 77 K, measured with a QWIP detector of 65 GHz band pass. Inset : Light current voltage characteristic of the microstrip laser operating at 77 K in cw. The shaded area corresponds to the operating point of the laser for the measurement of the modulation response.

2. Experimental results

2.1. Methods

The active region used for our experiments is an InGaAs/AlInAs QCL based on a two phonons design emitting around 9 μm [15, 16]. The device has been processed in a specific architecture for high frequency modulation [17]. The laser waveguide consists in a microstrip line. The optical mode is confined in a standard buried heterostructure [15], where the active region, etched in narrow ridges (8 μm), is embedded in two thick InP claddings (5 μm). Two gold layers are placed on the top and on the bottom of this waveguide. In this configuration the microwave signal propagates between two metal plates, along the dielectric stacks of the optical guide, enabling a good overlap of the modulation signal with the active region. On the other hand the thick InP layers enable negligible losses from the overlap of the optical mode with the metal layers. In Ref. [17] this device geometry demonstrated improved frequency response respect to standard lasers. In this work we exploit this property to injection lock the round trip frequency of the laser to a stable external RF source by direct modulation. To perform our experimental study the laser is mounted at the end of a 50 microstrip line and connected to it by short bonding wires. The modulation signal is supplied by a RF synthesizer (Anritsu MG3693B) through a Bias-T (SHF Communication Technologies BT45 B) and the optical signal is detected with an ultrafast QWIP of 65 GHz band pass [18]. The frequency response of the microstrip laser measured with this experimental set up is reported in Fig. 1. A flat response to direct modulation is demonstrated up to 14 GHz. Measurements at higher frequencies are limited by the circuit of our experimental set up. In the inset of the Fig. 1 is shown the light-current-voltage characteristic of the microstrip laser at 77 K in cw; the shaded area corresponds to the operating point of the laser for the measurement of the modulation response. The stability of the laser inter mode separation is estimated measuring the spectrum of the detected photocurrent in the microwave range, around the round-trip frequency. This signal is the beat note spectrum. The shape of this spectrum gives a direct access to the frequency and phase fluctuation of the modes separation due to the laser noise. Sharp single peak in the beat note spectrum proves a stable phase and frequency relation between neighboring laser modes. However it is not a conclusive proof of the generation of light pulses. Further investigation performing second order autocorrelation measurements is needed for this aim [19]. Deeper insight on the number of modes contributing to the beat note spectrum can be obtained from beat note spectroscopy measurements [14].

2.2. Results

In Fig. 2a we present the beat note spectra measured for different operating currents of the microstrip laser. A sharp single peak is observed at the round trip frequency (13.7324 GHz) in the all laser dynamic range ($J/J_{th} = 1.64$ corresponds to the maximum of the light output power, see inset Fig. 1). The peak width decreases from 200 kHz down to 100 kHz with increasing injected current. Comparing these results with standard buried heterostructures emitting at comparable wavelength ($\sim$9 μm), we find that the beat note of the microstrip laser is narrower than for standard devices [20]. As in laser diodes, stabilization of the laser modes could be related to saturable absorption effect present in our cavity [21]. However the relative large width of the microstrip waveguide excludes the effect of lossy sidewalls and Kerr lensing as locking mechanisms. In addition in Ref. [20] is demonstrated that saturable absorbers give characteristic laser spectra split in two groups,

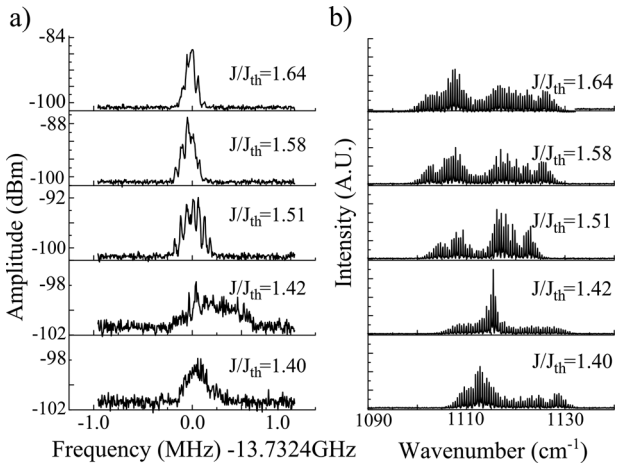

Figure 2 a) Measured RF spectra for different operating currents J/J_{th}; J_{th} is the threshold current. The frequency span is 2 MHz, the frequency resolution is 3 kHz. Each curve corresponds to an average over 100 measurements. b) Measured optical spectra for different operating currents with a resolution of 0.07 cm^{-1}.

whose frequency distance increases with the injected current. The optical spectra of the microstrip device are reported in Fig. 2b: the frequency emission has not a defined splitting and it slightly red-shifts with the increasing operating current. Measured narrow beat note spectra are related to the microstrip design of our device. Indeed, optical non linearities occurring within the QCL cavity can generate a microwave field that acts as a self-sustained modulation and couples the adjacent Fabry Perot modes. The origin of these non linearities is not evident yet, but we assume that they could be related to optical rectification in intersubbad transitions [22]. Therefore the reduced microwave losses as well as the increased overlap between the optical and RF modes favor the self-modulation and finally stabilize the inter-mode beating, as observed from experimental results.

In Fig. 3a we report the beat note spectra measured when the laser is directly modulated at a frequency 0.9 MHz apart from the round-trip frequency and operating at $J/J_{th} = 1.64$. Microwave spectra are presented in color scale (logarithmic scale) for different injected powers (corresponding to the y axis). Each single scan corresponds to an average over 100 measurements with a resolution bandwidth of 10 kHz; the signal has been normalized for the background noise measured blocking the laser light with a cardboard. The same experimental conditions have been used for all the beat note spectra measurements presented in this work. From these results we see that when the microwave injected power P is low (–5 dBm <P< 0 dBm) the spectral position of the beat note stays constant. Most of signal intensity is concentrated on the beat note with a small part at the injected frequency. For 0 dBm < P < 7 dBm the intensity of the beat note starts to decrease and its central frequency moves toward the injected RF frequency, until it reaches an instability region. At the same time a clear sideband appears on the right side of the spectrum. By further increase of the injected power, the beat note becomes a single narrow peak.

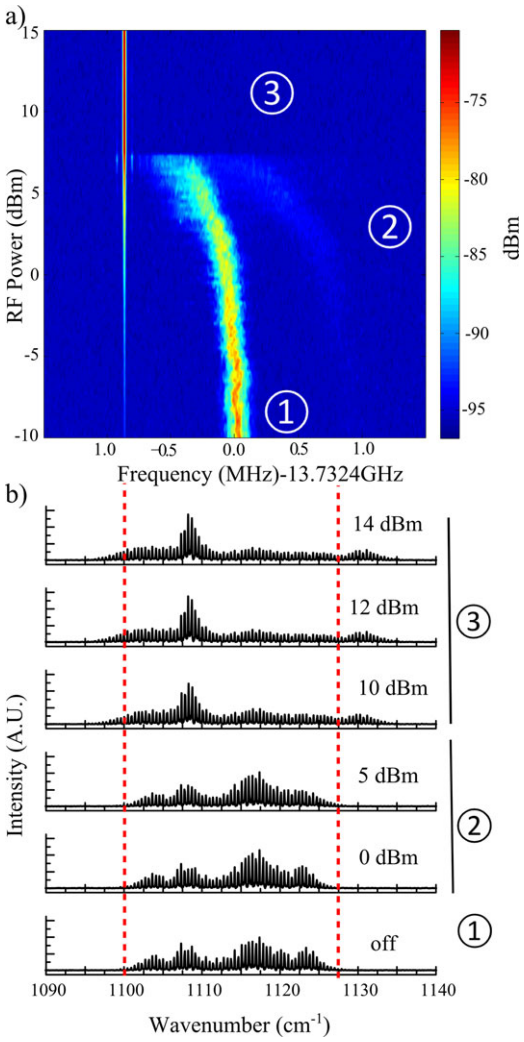

Figure 3 a) Measurement of the beat note spectra of the microstrip QCL for different RF injected powers. The RF frequency is set 0.9 MHz apart from the cavity round trip frequency and the laser is operating at the maximum of the light current curve ($J/J_{th} = 1.64$). On the Y-axis is reported the RF injected power delivered by the external synthesizer (power step of 0.25 dBm) and on the X-axis the frequency of the signal on the spectrum analyzer, renormalized with an offset at the round trip frequency. In color scale is the intensity of the measured RF signal (dBm). Each single scan corresponds to an average over 100 measurements; the resolution bandwidth is 10 kHz. (b) Optical spectrum as function of the RF injected power and without injection measured with a resolution of 0.07 cm^{-1}.

Tuning of the beating frequency of ∼1 MHz with 7 dBm (5 mW) of injected power (all the set up losses are neglected) is reported. In Fig. 3b the optical spectra for different RF injected power, measured in the same condition of Fig. 3a are presented. A broadening of the optical spectrum of 13 cm^{-1} (40% increase) is demonstrated. This is related to the microwave injection that generates side bands of the free running modes, and an increased number of frequencies is brought above threshold within the gain curve.

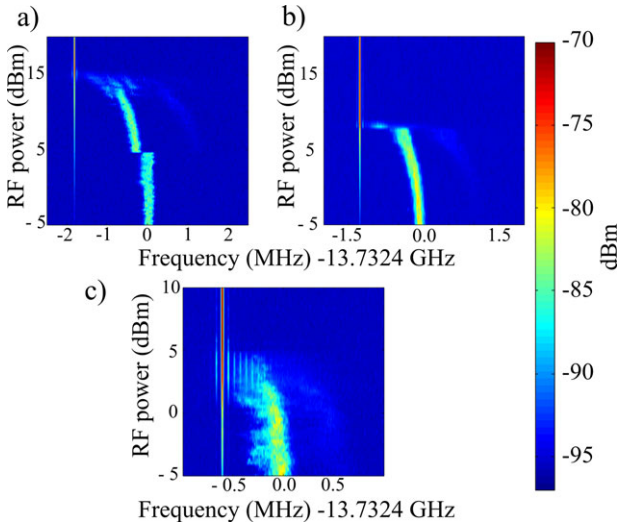

Figure 4 Measurement of the RF spectra for the microstrip QCL for different RF injected powers. The laser is operating at the maximum of the light current curve ($J/J_{th} = 1.64$). The RF frequency is set 1.8 MHz (a) 1.2 MHz (b) and 0.6 MHz (c) apart from the cavity round trip frequency. Each single scan corresponds to an average over 100 measurements with a resolution bandwidth of 10 kHz.

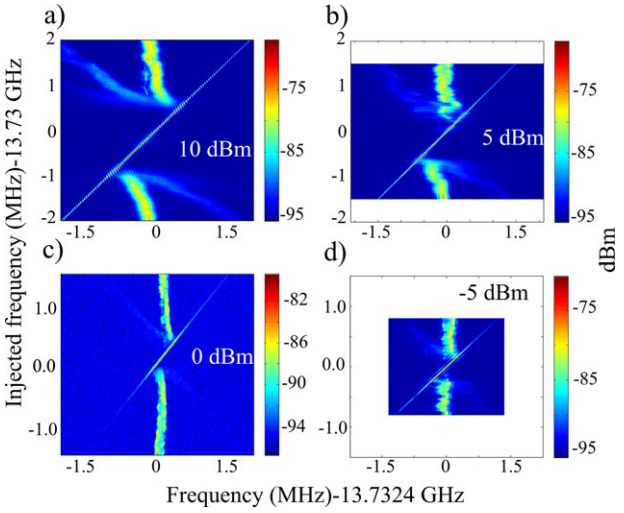

Figure 5 Measurement of the RF spectra for the microstrip QCL for different RF injected frequencies. The laser is operating at the maximum of the light current curve ($J/J_{th} = 1.64$). The RF power is set to 10 dBm (a), 5 dBm (b), 0 dBm (c) and –5 dBm (d). The experimental conditions are the same of Fig. 3a. On the Y-axis is reported the RF injected frequency and on the X-axis the frequency of the signal on the spectrum analyzer, renormalized with an offset at the round trip frequency. In color scale is the intensity of the measured RF signal (dBm). Each single scan corresponds to an average over 100 measurements; the resolution bandwidth is 10 kHz.

As systematic study of the injection locking dynamics, different measurements of the beat note spectra as function of the injected RF power have been performed; results are reported in Fig. 4. The frequency distance between the beat note and the driving signal is 1.8 MHz, 1.2 MHz and 0.6 MHz respectively for panel a, b and c. From these results we see that the general behavior of the injection is the same as discussed above, regardless of the frequency distance. However, the further the frequency separation, the higher is the power needed to reach locking and to see the sidebands appearing. Instability regions are visible in the three sets of measurements.

In order to have a deeper insight on the frequency locking range and on the unlocking processes, we performed a second set of measurements and results are presented in Fig. 5. The RF spectra (color scale) in this case have been measured for different injected frequencies (reported on the y axis) and fixed value of the power: 10 dBm, 5 dBm, 0 dBm and –5 dBm respectively for panel a,b,c,d. Measurements have been performed by changing the injected frequency from lower to higher values. As the driving frequency approaches the free running beat note, the spectra move toward this value until the whole intensity is concentrated in a single narrow peak. Locking is reached and the spectra are controlled by the external injected signal. By further increasing the RF frequency the spectra start to broaden and split in two separate peaks, coming back to the same shape and position measured at the beginning of experience (bottom part of the graph). The region where a single narrow peak is measured corresponds to the measured locking range. All the results presented are in agreement with the classical theory of injection locking, as we will show in more details in the following section.

3. Theory and comparison with experimental results

As proposed in Ref. [11] for THz QCL and as widely used for conventional laser system [1], stabilization of the laser oscillation through the injection of an external stable signal, can be studied using the formalism of injection locked coupled oscillators. This approach describes the interaction of two oscillators where one is a self-sustained system and the other is a weak perturbation signal. It has been successfully implemented for electrical and optical systems, giving similar results [1, 2].

Considering the optical case, injection locking model depicts a scheme where a master laser oscillating at a frequency ω_1 is injected in a slave laser oscillating at a free-running frequency ω_0, close to ω_1. The signal at ω_1, circulating in the cavity, can be regeneratively amplified by the gain, which is clamped for ω_0 but not for ω_1. At a certain point the amplified intensity at ω_1 begins to approach the value of the initial optical intensity at ω_0 and it can begin to saturate the laser gain to suppress the oscillation at ω_0.

In more details, following the formalism of Ref. [1], if a field $E_1 e^{[i\omega_1 t]}$ is injected in the laser, where the cavity mode is $E_0 e^{i[\omega_1 t+\varphi(t)]}$, the equations describing radiation matter interaction can be written in the phase-amplitude

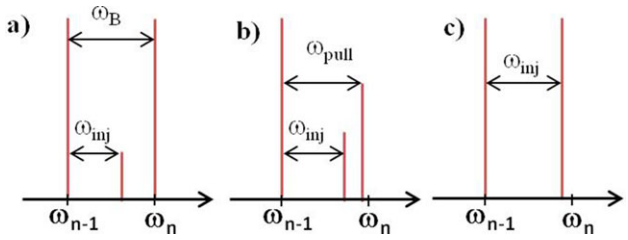

Figure 6 Schematic of the direct microwave modulation of a laser. Injected microwave frequency outside the locking range (a), close to the locking range (b) and in the locking range (c).

form and, in the approximation of weak injection, only the phase equation can be considered:

$$\frac{d\varphi}{dt} = \omega_0 - \omega_1 - \frac{\omega_0}{Q}\frac{E_1}{E_0}\sin\varphi \tag{1}$$

where Q is the cavity quality factor.

Analytic solutions can be found for two limiting cases. When ω_1 belongs to a specific frequency range, defined as locking range, the injected signal locks the cavity mode: ω_0 is suppressed and time varying component of the phase φ is zero. By setting $\frac{d\varphi}{dt} = 0$ in Eq. (1) and imposing $-1 < \sin\varphi < 1$ the locking range ω_m can be written as:

$$\omega_m = \frac{\omega_0}{Q}\sqrt{\frac{I_1}{I_0}} \tag{2}$$

where I_1 and I_0 are the injected signal and the cavity signal intensities, respectively. With this definition the full frequency range in which the system is locked by ω_1 is $2\omega_m$.

In the case of ω_1 close, but not in the locking range, the oscillating frequency in the cavity moves from ω_0 to a close frequency ω_{osc}, pulled toward the injection.

$$\omega_{osc} = \omega_0 + \frac{\omega_0^2}{2Q^2(\omega_1 - \omega_0)}\frac{I_1}{I_0} \tag{3}$$

In this work we have adapted these results to the direct modulation of a QCL by interpreting the system according to the following scheme (See Fig. 6). In a Fabry-Perot cavity, laser modes oscillate at frequencies ω_n, separated by the round-trip frequency ω_B, within the width $\delta\omega$, representing their frequency and phase noise. In the steady state situation, before the injection of the external signal, the laser gain is clamped at the losses value. When an external modulation at ω_{inj} is applied to the laser, lateral sidebands at frequencies $\omega_n \pm \omega_{inj}$ are created.

Starting from two neighbor modes the sideband of the mode ω_{n-1} at the frequency $\omega_{n-1} + \omega_{inj}$ can be regeneratively amplified and take over the mode at ω_n.

Two modes are locked together within a noise width given by the external source and $\ll\delta\omega$. Starting from these modes the same process can repeat all along the gain curve until the system reaches a stable configuration. In this picture the cavity field E_0 is the field at ω_n and the injected electric field E_1 is the field at $\omega_{n-1} + \omega_{inj}$. The last term is $E_{inj}/\sqrt{a}$ where E_{inj} is the injected microwave signal and a is a constant taking in account the losses of the modulation signal coming from the impedance mismatch at the laser input and from the cavity. Within this picture, Eqs. (1) and (2) can be written as:

$$\frac{d\varphi}{dt} = \omega_B - \omega_{inj} - \frac{\omega_n}{Q}\frac{E_{inj}}{E_0\sqrt{a}}\sin\varphi \tag{4}$$

$$\omega_m = \frac{\omega_n}{Q}\sqrt{\frac{I_{inj}}{aI_0}} \tag{5}$$

When the modulation frequency is outside the locking range, but close to it, the separation between the longitudinal modes of the laser is not anymore ω_B but ω_{pull} (See Fig. 6b) and Eq. (3) is written as:

$$\omega_{pull} - \omega_B = \frac{\omega_n^2}{2Q^2(\omega_{inj} - \omega_B)}\frac{I_{inj}}{aI_0} \tag{6}$$

In this work we found numeric solution of Eq. (4) for different locking ranges and frequencies of the injected signal. From these solutions the spectrum of the cavity field has been found by Fourier transform of the expression $E_0 e^{i[\omega_1 t + \varphi(t)]}$ presented above. In Fig. 7a we present the calculated spectra of the cavity field for a fixed injected frequency and increasing value of the locking range.

From Eq. (5), this is equivalent to increase of the modulation signal intensity; these theoretical results can then be compared to experimental spectra presented in Figs. 3a–4. While ω_{inj} approaches the locking range the intensity at ω_B decreases and an increasing number of more intense sidebands is visible. When ω_{inj} is extremely close to the locking range an instability region is observed; further increase of the locking range brings all emission spectrum to the injected frequency. All these features are in good agreement with experimental results. Only a limited number of sidebands is however visible in Figs. 3a–4; this is probably due to the limited signal to noise value of our set up.

The injection locking model has been further proved by comparison of the experimental results on the beat note spectra for different injected power (Figs. 3a–4) with their expected central frequency predicted in Eq. (6). Gaussian fits of the experimental spectra presented in Figs. 3a and 4 were performed to estimate the frequency position of the beat note (ω_{pull}). Plotting these values as function of the injected power (Fig. 7b) we find a linear relation, as predicted from Eq. (6). Values of the slope of each linear fit are then displayed as function of $1/(\omega_B - \omega_{inj})$; good agreement with the expected linear relation is demonstrated in Fig. 7c.

Similar results are obtained for the numerical calculation of the spectra of the cavity field calculated fixing the locking range and changing the injection frequency (Fig. 8a); these results are in good agreement with experiments (Fig. 5). In addition an estimate of the measured

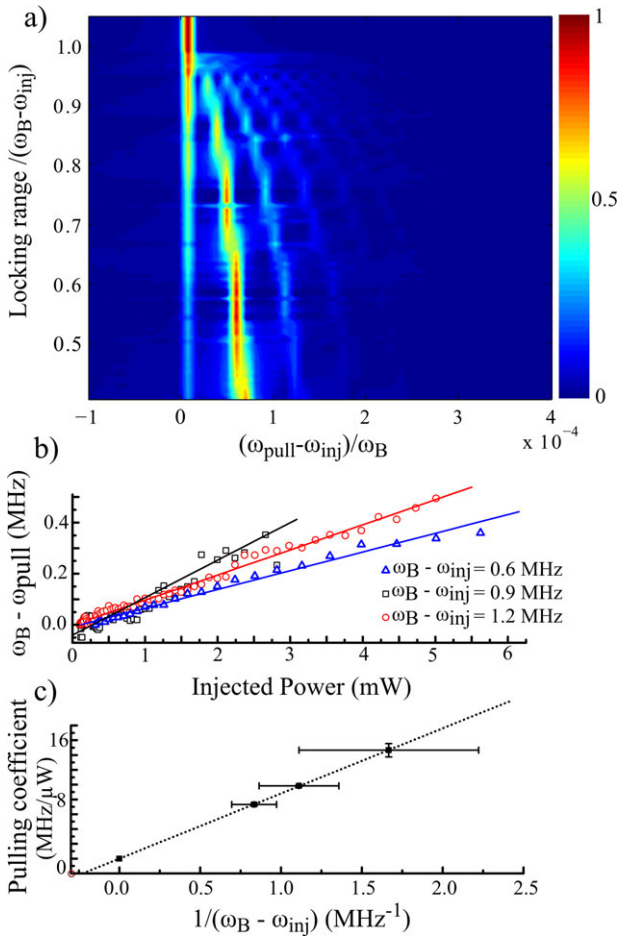

Figure 7 a) Results of numerical calculation of the injection locking equation. The system is supposed to oscillate at the initial frequency ω_B and to be perturbed by a signal at $\omega_{inj.}$ The locking range frequency of the system is varied and reported on the Y axis. On the X axis is reported the frequency of the calculated spectra $\omega_{pull} - \omega_{inj}\ /\omega_B$. In Figure b) and c) the comparison of the experimental results with the injection locking theory is reported. b) Study of the beat note peak position for different values of $\omega_B - \omega_{inj}$. Values of the peak position are estimated from experimental data reported in Figs. 3a–4b,c and they are reported as function of the injected microwave power with an offset and the frequency of the unperturbed beat note ω_B. Lines correspond to separate linear fit of each data set. c) The slope of the linear fit presented in b) are reported as function of $1/\omega_B - \omega_{inj}$. Dotted line corresponds to a linear fit of the data

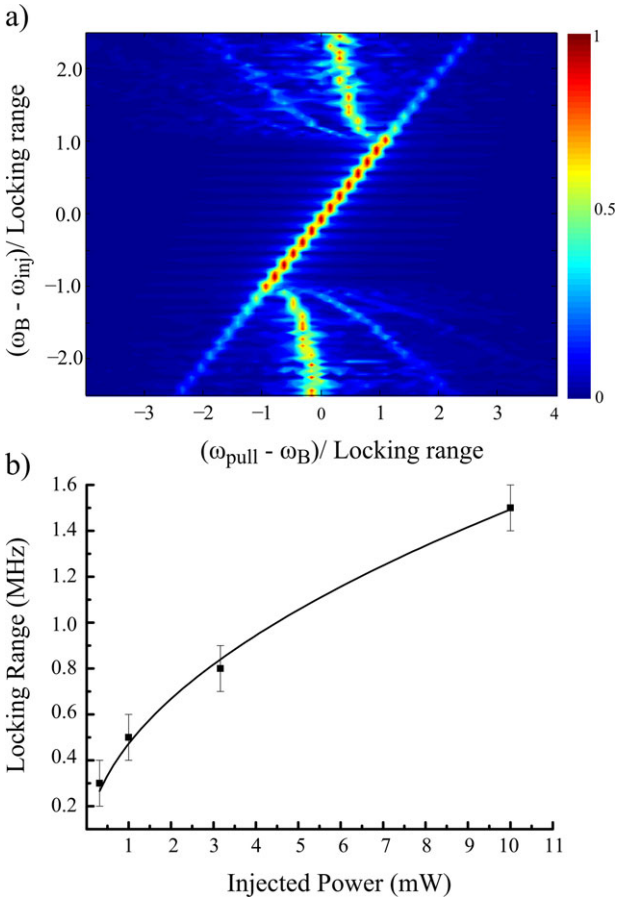

Figure 8 a) Results of numerical calculation of the injection locking equation. The system is supposed to have a fixed locking range, to oscillate at the initial frequency ω_B and to be perturbed by a signal at $\omega_{inj.}$ The frequency ω_{inj} of the external signal is varied and reported on the Y axis with an offset at ω_B and normalized by the given locking range. On the X axis is reported the frequency of the calculated spectra $\omega_{pull} - \omega_{inj}$/Locking range. b) Measured locking range for different injected modulation power intensities. These values are estimated from the experimental data of Fig. 5 and are reported as function of the injected power. Line corresponds to a square root fit of the experimental data.

locking range from data in Fig. 5 has been done and results are reported as function of the injected power in Fig. 8b. As predicted from Eq. (5) the experimental results follow a square root fit as function of the injected power.

4. Conclusions

In this work direct modulation of a QCL laser emitting at 9 μm is studied. Designing a device architecture where the laser cavity is embedded in a microstrip line, injection locking to a stable microwave source at 13.7 GHz over ~2 MHz is demonstrated. A good agreement with the theory of locking for two coupled oscillators is demonstrated.

Received: 21 November 2013, **Revised:** 31 January 2014, **Accepted:** 14 February 2014

Published online: 21 March 2014

Key words: mid-infrared quantum cascade lasers, high frequency modulation, injection locking.

References

[1] A. E. Siegman, Lasers (University Science Books, 1986), Chapter 29.

[2] B. Razavi, IEEE J. Sol. State Circuits. **39**(9), 1415–1424 (2004).
[3] O. Lidoyne, P. B. Gallion, and D. Erasme, IEEE J. Quantum Electron. **27**, 344–351(1991).
[4] Z. Ahmed, L. Zhai, A. J. Lowery, N. Onodera, and S. Tucker Rodney, IEEE J. Quantum Electron. **29**, 1714–1721 (1993).
[5] E. J. Ripper and L. T. Paoli, Appl. Phys. Lett. **15**, 203–205 (1969).
[6] T. B. Simpson, J. M. Liu, K. F. Huang, and K. Tai, J. Eur. Opt. Soc Part B **9**, 765–784 (1997).
[7] A. Yariv and P. Yeh, Photonics, (Oxford University, 2007), Chapter 15.
[8] I. Freitag and H. Welling, Appl. Phys. B **58**, 537 (1994).
[9] J. Faist, Quantum Cascade Lasers (Oxford University, 2013), Chapter 12.
[10] B. Meng and Q. Wang, Opt. Express **20**, 1450–1464 (2012).
[11] P. Gellie, S. Barbieri, J. Lampin, P. Filloux, C. Manquest, C. Sirtori, I. Sagnes, S. Khanna, E. Linfield, A. Davies, H. Beere, and D. Ritchie, Opt. Express **18**, 20799–20816 (2010).
[12] A. Baryshev, J. N. Hovenier, A. J. L. Adam, I. Kasalynas, J. R. Gao, T. O. Klaassen, B. S. Williams, S. Kumar, Q. Hu, and J. L. Reno, Appl. Phys. Lett. **89**, 031115 (2006).
[13] R. Paiella, F. Capasso, C. Gmachl, H. Y. Hwang, D. L. Sivco, A. L. Hutchinson, A. Y. Cho, and H. C. Liu, Appl. Phys. Lett. **77**, 169 (2000).
[14] A. Hugi, G. Villares, S. Blaser, H. C. Liu, and J. Faist, Nature **492**, 229–233 (2012).
[15] M. Beck, D. Hofstetter, T. Aellen, J. Faist, U. Oesterle, M. Ilegems, E. Gini, and H. Melchior, Science **295**, 301 (2002).
[16] A. Wittmann, Y. Bonetti, M. Fischer, J. Faist, S. Blaser, and E. Gini, IEEE Photon. Technol. Lett. **21**, 814 (2009).
[17] A. Calvar, M. I. Amanti, M. Renaudat St-Jean, S. Barbieri, A. Bismuto, E. Gini, M. Beck, J. Faist, and C. Sirtori, Appl. Phys. Lett. **102**, 181114 (2013).
[18] H. C. Liu, R. Dudek, T. Oogarah, P. D. Grant, Z. R. Wasilewski, H. Schneider, S. Steinkogler, M. Walther, and P. Koidl, Circuits and Devices Magazine, IEEE **19**, 9–16, (2003).
[19] C. Wang, L. Kuznetsova, V. Gkortsas, L. Diehl, F. Kärtner, M. Belkin, A. Belyanin, X. Li, D. Ham, H. Schneider, P. Grant, C. Song, S. Haffouz, Z. Wasilewski, H. Liu, and F. Capasso, Opt. Express **17**, 12929–12943 (2009).
[20] A. Gordon, C. Y. Wang, L. Diehl, F. X. Kärtner1, A. Belyanin, D. Bour, S. Corzine, G. Höfler, H. C. Liu, H. Schneider, T. Maier, M. Troccoli, J. Faist, and F. Capasso, Phys. Rev. A **77**, 053804, 1–18 (2008).
[21] C. R. Mirasso, G. H. M. Van Tartwijk, E. Hernandez-Garcia, D. Lenstra, S. Lynch, P. Landais, P. Phelan, J. O'Gorman, M. San Miguel, and W. Elsasser, IEEE J. Quantum Electron. **35**, 764–770 (1999).
[22] E. Dupont, Z. R. Wasilewski, and H. C. Liu, IEEE J. Quantum Electron. **42**, 1157–1174 (2006).